PHYSICAL REVIEW D **88,** 054023 (2013)

Sivers effect and the single spin asymmetry A_N in $p^\uparrow p \to hX$ processes

M. Anselmino,[1,2] M. Boglione,[1,2] U. D'Alesio,[3,4] S. Melis,[1,2] F. Murgia,[4] and A. Prokudin[5]
[1]*Dipartimento di Fisica Teorica, Università di Torino, Via P. Giuria 1, I-10125 Torino, Italy*
[2]*INFN, Sezione di Torino, Via P. Giuria 1, I-10125 Torino, Italy*
[3]*Dipartimento di Fisica, Università di Cagliari, Cittadella Universitaria, I-09042 Monserrato (CA), Italy*
[4]*INFN, Sezione di Cagliari, C.P. 170, I-09042 Monserrato (CA), Italy*
[5]*Jefferson Laboratory, 12000 Jefferson Avenue, Newport News, Virginia 23606, USA*
(Received 6 May 2013; published 23 September 2013)

The single spin asymmetry A_N, for large P_T single inclusive particle production in $p^\uparrow p$ collisions, is considered within a generalized parton model and a transverse momentum dependent factorization scheme. The focus is on the Sivers effect and the study of its potential contribution to A_N, based on a careful analysis of the Sivers functions extracted from azimuthal asymmetries in semi-inclusive deep inelastic scattering processes. It is found that such Sivers functions could explain most features of the A_N data, including some recent STAR results which show the persistence of a nonzero A_N up to surprisingly large P_T values.

DOI: 10.1103/PhysRevD.88.054023 PACS numbers: 13.88.+e, 12.38.Bx, 13.85.Ni

I. INTRODUCTION

Among the leading-twist transverse momentum dependent partonic distribution functions (TMD-PDFs, often shortly referred to as TMDs), the Sivers distribution [1–3] is most interesting and widely investigated. It describes the number density of unpolarized quarks q (or gluons) with intrinsic transverse momentum $\boldsymbol{k}_\perp$ inside a transversely polarized proton $p^\uparrow$, with three-momentum $\boldsymbol{P}$ and spin polarization vector $\boldsymbol{S}$,

$$\hat{f}_{q/p^\uparrow}(x,\boldsymbol{k}_\perp) = f_{q/p}(x,k_\perp) + \frac{1}{2}\Delta^N f_{q/p^\uparrow}(x,k_\perp)\boldsymbol{S}\cdot(\hat{\boldsymbol{P}}\times\hat{\boldsymbol{k}}_\perp), \tag{1}$$

where x is the proton light-cone momentum fraction carried by the quark, $f_{q/p}(x,k_\perp)$ is the unpolarized TMD ($k_\perp = |\boldsymbol{k}_\perp|$) and $\Delta^N f_{q/p^\uparrow}(x,k_\perp)$ is the Sivers function. $\hat{\boldsymbol{P}} = \boldsymbol{P}/|\boldsymbol{P}|$ and $\hat{\boldsymbol{k}}_\perp = \boldsymbol{k}_\perp/k_\perp$ are unit vectors. Notice that the Sivers function is most often denoted as $f_{1T}^{\perp q}(x,k_\perp)$ [4]; this notation is related to ours by [5]

$$\Delta^N f_{q/p^\uparrow}(x,k_\perp) = -\frac{2k_\perp}{m_p} f_{1T}^{\perp q}(x,k_\perp). \tag{2}$$

A knowledge of the Sivers distribution allows a modeling of the three-dimensional momentum structure of the nucleon [6] and, possibly, an estimate of the parton orbital angular momentum [7].

All the available information on the Sivers function has been obtained from SIDIS data, $\ell N \to \ell h X$, and the study of the azimuthal distribution of the final hadron h around the γ^* direction in the $\gamma^* - N$ center of mass (c.m.) frame. This analysis is based on the TMD factorization scheme [8–11], according to which the SIDIS cross section is written as a convolution of TMD-PDFs, transverse momentum dependent fragmentation functions (TMD-FFs) and known elementary interactions. Such a scheme holds in the kinematical region defined by

$$P_T \simeq k_\perp \simeq \Lambda_{\rm QCD} \ll Q, \tag{3}$$

where P_T is the magnitude of the final hadron transverse momentum. The presence of the two scales, small P_T and large Q, allows one to identify the contribution from the unintegrated partonic distributions ($P_T \simeq k_\perp$), while remaining in the region of validity of the QCD parton model. The study of the QCD evolution of the Sivers and unpolarized TMDs—the so-called TMD evolution—has much progressed lately [8,9,11–15], with the first phenomenological applications [16–22].

The extraction of the Sivers functions from SIDIS data can then be performed on a sound ground. This has been done for the first time in Refs. [23–27], exploiting HERMES [28] and COMPASS [29] data, and resulting in a reasonable knowledge of the Sivers functions for u and d quarks, although in a limited range of x values, $x \lesssim 0.3$.

Much literature has emphasized the special interest and the peculiar properties of the Sivers effect. Trying to understand its origin at the partonic level has related the possibility of a nonzero Sivers function with final [30] or initial [31] state interactions, respectively, in SIDIS and Drell-Yan (D-Y) processes. This, in turn, induces a process dependence of the effect itself. The most clear-cut consequence is the prediction of an opposite sign of the Sivers functions when contributing to single spin asymmetries (SSAs) in SIDIS and D-Y processes [32]; as polarized D-Y experiments have never been performed so far, such a prediction has not been tested yet. Crucial information might be available in the future from $p^\uparrow p$ experiments at RHIC and Fermilab or from the COMPASS hadronic run at CERN, with pions colliding on a polarized nucleon target. The TMD factorization scheme, valid for SIDIS processes, holds for D-Y as well, where the small and large scales are, respectively, the total transverse momentum (q_T) and the invariant mass (M) of the leptonic pair.

In this paper we focus on another class of puzzling results that strongly challenge our understanding of high

energy strong interactions, that is the SSAs, usually denoted by A_N, measured in $p^\uparrow p \to hX$ inclusive reactions and defined as

$$A_N = \frac{d\sigma^\uparrow - d\sigma^\downarrow}{d\sigma^\uparrow + d\sigma^\downarrow} \quad \text{with} \quad d\sigma^{\uparrow,\downarrow} \equiv \frac{E_h d\sigma^{p^{\uparrow,\downarrow}p\to hX}}{d^3\boldsymbol{p}_h}, \quad (4)$$

and where $\uparrow, \downarrow$ are opposite spin orientations perpendicular to the scattering plane, in the $p^\uparrow p$ c.m. frame. A_N differs from the SSAs of SIDIS and D-Y processes because in such a case there is only one large scale in the process—the transverse momentum P_T of the final observed hadron—and there is no small scale related to the intrinsic motions, in both the distribution and fragmentation functions, which are integrated over. The TMD factorization scheme used for SIDIS and D-Y processes has not been proven in this case.

Large values of A_N have been measured for a long time in many different experiments. The first ones were at a relatively low energy [33–40], and the common expectation was that such asymmetries would vanish at higher energies; however, data from RHIC at $\sqrt{s} = 62.4$ [41], 200 [42–46] or even 500 [47,48] GeV, still show puzzling nonzero values of A_N.

Several approaches to understanding A_N, within QCD and some sort of factorization scheme, can be found in the literature. All of them, directly or indirectly, are related to the Sivers function or other TMDs.

A QCD collinear factorization formalism at next-to-leading power (twist-3) has been developed and used in the phenomenological studies of A_N [49–57]. In this approach the spin effect is not embedded in a spin dependent TMD, but the necessary phase for generating the nonvanishing SSAs arises from the quantum interference between an elementary scattering amplitude with one active collinear parton and an amplitude with two active collinear partons. The SSAs are therefore proportional to some nonprobabilistic three-parton correlation functions, which are convoluted with the product of amplitudes, rather than the cross sections. These amplitudes are process dependent, while the three-parton correlation functions are universal.

However, one can show that the twist-3 three-parton correlation functions have a close connection with the $k_\perp$ moment of the TMD-PDFs; in particular the quark-gluon correlator is related to the first $k_\perp$ moment of the SIDIS Sivers function [58]. It has recently been pointed out [59] that the quark-gluon correlation functions, as obtained from the Sivers functions extracted from SIDIS data [23,24], indeed lead to sizable values of A_N, which agree in magnitude with the measured ones, but *with the wrong sign* (the so-called sign mismatch problem). A recent analysis [60] of the spin asymmetry A_N for single inclusive jet production in $p^\uparrow p$ collisions collected by the A_NDY experiment [61] does not show the same sign problem; however, the measured asymmetry is very small.

An alternative, more phenomenological approach, is based on the assumption of the validity of the TMD factorization also for $p^\uparrow p \to hX$ processes [1,2,62–67]; it generalizes the usual collinear factorization scheme [generalized parton model (GPM)] and the single inclusive cross section is written as a convolution of TMD-PDFs, TMD-FFs and QCD partonic cross sections. In that it adopts the same scheme that holds for SIDIS and D-Y processes with one small and one large scale. In this model the spin effects are included in the TMDs, which are supposed to be process independent.

More recently, a third approach has been proposed [68,69], which assumes the TMD factorization as in the GPM, but takes into account and absorbs the initial and final state interactions, i.e. the process dependence of the Sivers function, in the elementary interactions. In such a scheme the cross section is a convolution of process-independent TMDs with process-dependent hard parts; these modified hard parts are very similar in form to those in the twist-3 collinear approach. It turns out that this modified GPM formalism leads to results and predictions opposite to those of the conventional GPM [68].

In this paper we explore the possibility of understanding the experimental results on A_N in $p^\uparrow p \to hX$ processes with the Sivers effect and within the generalized parton model of Refs. [65–67]. The first phenomenological applications of the Sivers effect [62,63,65] in hadronic interactions considered the Sivers function as a free input, not constrained by SIDIS data. In Ref. [70] it was shown that the use of the Sivers functions, as extracted from SIDIS data, could in principle explain the SSAs observed at RHIC, both in size and in sign. We further pursue this study, with a careful analysis of the SIDIS extracted Sivers functions, with their uncertainties, and investigate whether such functions, assumed to be process independent, can explain the data on A_N, including the most recent ones. A similar study has been recently completed [71] regarding the Collins effect [72], with the conclusion that it cannot, alone, explain all the available data on A_N.

II. SIVERS EFFECT AND A_N IN THE GENERALIZED PARTON MODEL FORMALISM

The generalized parton model [65–67,71] can be considered as a natural phenomenological extension of the usual collinear factorization scheme, with the inclusion of spin and $k_\perp$ effects through the TMDs and the dependence of the elementary interactions on the parton intrinsic motions; it was actually first proposed, for unpolarized processes, in Ref. [73]. In this approach the single spin effect, $d\sigma^\uparrow \neq d\sigma^\downarrow$, originates from the TMDs; in Ref. [74] and its correction [71] it was shown that the only non-negligible contributions to A_N are given by the Sivers TMD-PDF and the Collins TMD-FF,

$$A_N = \frac{[d\sigma^\uparrow - d\sigma^\downarrow]_{\text{Sivers}} + [d\sigma^\uparrow - d\sigma^\downarrow]_{\text{Collins}}}{d\sigma^\uparrow + d\sigma^\downarrow}. \quad (5)$$

The Collins contribution was studied in Ref. [71], while this paper is devoted to the Sivers effect.

In our GPM scheme the contribution of the Sivers effect to the numerator of A_N, for $p^\uparrow p \to hX$ large P_T processes, is given by

$$[d\sigma^\uparrow - d\sigma^\downarrow]_{\rm Sivers} = \sum_{a,b,c,d} \int \frac{dx_a dx_b dz}{16\pi^2 x_a x_b z^2 s} d^2\boldsymbol{k}_{\perp a} d^2\boldsymbol{k}_{\perp b} d^3\boldsymbol{p}_\perp \delta(\boldsymbol{p}_\perp \cdot \hat{\boldsymbol{p}}_c) J(p_\perp) \delta(\hat{s} + \hat{t} + \hat{u}) \times \Delta^N f_{a/p^\uparrow}(x_a, k_{\perp a}) \cos(\phi_a) f_{b/p}(x_b, k_{\perp b}) \frac{1}{2} [|\hat{M}_1^0|^2 + |\hat{M}_2^0|^2 + |\hat{M}_3^0|^2]_{ab\to cd} D_{h/c}(z, p_\perp), \quad (6)$$

where $\Delta^N f_{a/p^\uparrow}(x_a, k_{\perp a})$ is the Sivers function for parton a, Eqs. (1) and (2), which couples to the unpolarized TMD for parton b, $f_{b/p}(x_b, k_{\perp b})$, and the unpolarized fragmentation function $D_{h/c}(z, p_\perp)$ of parton c into the final observed hadron h. $\boldsymbol{p}_\perp$ is the transverse momentum of hadron h with respect to the 3-momentum $\boldsymbol{p}_c$ of its parent fragmenting parton. $J(p_\perp)$ is a kinematical factor, which at $\mathcal{O}(p_\perp/E_h)$ equals 1. For details and a full explanation of the notations we refer to Ref. [66] (where $\boldsymbol{p}_\perp$ is denoted as $\boldsymbol{k}_{\perp C}$).

The phase factor $\cos(\phi_a)$ originates directly from the $\boldsymbol{k}_\perp$ dependence of the Sivers distribution [$\boldsymbol{S} \cdot (\hat{\boldsymbol{P}} \times \hat{\boldsymbol{k}}_\perp)$, Eq. (1)], while the $\hat{M}_i^0$ are the three independent hard scattering helicity amplitudes defined in Ref. [66], describing the lowest order QCD interactions. The sum of their moduli squared is proportional to the elementary unpolarized cross section $d\hat{\sigma}^{ab\to cd}$, that is

$$\frac{d\hat{\sigma}^{ab\to cd}}{d\hat{t}} = \frac{1}{16\pi\hat{s}^2} \frac{1}{2} \sum_{i=1}^{3} |\hat{M}_i^0|^2. \quad (7)$$

The explicit expressions of $\sum_i |\hat{M}_i^0|^2$, which give the QCD dynamics in Eq. (6), can be found, for all possible elementary interactions, in Ref. [66]. The QCD scale is chosen as $Q = P_T$.

The denominator of Eq. (4) or (5) is twice the unpolarized cross section and is given in our TMD factorization by the same expression as in Eq. (6), where one simply replaces the factor $\Delta^N f_{a/p^\uparrow} \cos(\phi_a)$ with $2 f_{a/p}$. In Ref. [70] it was shown that such an expression leads to results for the unpolarized cross section in agreement with data.

We can now use the information so far available on the Sivers functions as extracted from SIDIS data and give some realistic estimates for the Sivers contribution to A_N for several single-inclusive large P_T particle production in $p^\uparrow p$ collisions. More specifically, we will consider the Sivers effect for inclusive pion, kaon, photon and jet production and will see how much it can contribute to the available experimental data on A_N. The analogue of Eq. (6) for direct photon and inclusive jet production will be given below.

A. The Sivers functions in SIDIS and $p^\uparrow p \to hX$ processes

Let us start by considering the available information on the Sivers functions and the procedure followed to obtain them. The first extraction—from now on denoted as the SIDIS-1 fit—was presented in Ref. [23], where the MRST01 set for the unpolarized PDFs [75] and the Kretzer set for the unpolarized FFs [76] were adopted. An updated extraction of the Sivers functions—SIDIS-2 fit—was presented in Ref. [24]. In this case, the GRV98 set for the unpolarized PDFs [77] and the pion and kaon FFs by de Florian, Sassot and Stratmann (DSS) [78] were considered. Notice that the use of different PDFs does not make any relevant difference; therefore, in the following, we will consider only the GRV98 set.

The main features of the parametrizations adopted in those studies are the following: the analysis of SIDIS data is performed at leading order, $\mathcal{O}(k_\perp/Q)$, within the proven TMD factorization approach for SIDIS, where Q is the large scale in the process. A simple factorized form of the TMD functions was adopted, using a Gaussian shape for their $k_\perp$ dependent component. For the unpolarized parton distribution and fragmentation functions we have

$$f_{q/p}(x, k_\perp) = f_{q/p}(x) \frac{e^{-k_\perp^2/\langle k_\perp^2\rangle}}{\pi\langle k_\perp^2\rangle}, \qquad D_{h/q}(z, p_\perp) = D_{h/q}(z) \frac{e^{-p_\perp^2/\langle p_\perp^2\rangle}}{\pi\langle p_\perp^2\rangle}, \quad (8)$$

where $\langle k_\perp^2\rangle$ and $\langle p_\perp^2\rangle$ have been fixed by analyzing the Cahn effect in unpolarized SIDIS processes (see Ref. [79]):

$$\langle k_\perp^2\rangle = 0.25\ \text{GeV}^2, \qquad \langle p_\perp^2\rangle = 0.20\ \text{GeV}^2. \quad (9)$$

The recently introduced TMD evolution was not taken into account, while we considered the DGLAP QCD evolution of the collinear factorized part.

The Sivers functions, $\Delta^N f_{q/p^\uparrow}(x, k_\perp)$, have been parametrized as follows:

$$\Delta^N f_{q/p^\uparrow}(x, k_\perp) = 2\mathcal{N}_q^S(x) f_{q/p}(x) h(k_\perp) \frac{e^{-k_\perp^2/\langle k_\perp^2\rangle}}{\pi\langle k_\perp^2\rangle}, \quad (10)$$

where

$$\mathcal{N}_q^S(x) = N_q^S x^{\alpha_q} (1-x)^{\beta_q} \frac{(\alpha_q + \beta_q)^{(\alpha_q+\beta_q)}}{\alpha_q^{\alpha_q} \beta_q^{\beta_q}}, \quad (11)$$

with $|N_q^S| \le 1$, and

$$h(k_\perp) = \sqrt{2e}\,\frac{k_\perp}{M}\,e^{-k_\perp^2/M^2}. \tag{12}$$

With these choices, the Sivers functions automatically fulfill their proper positivity bounds for any $(x, k_\perp)$ values. For the Q^2 evolution of the Sivers function, as commented above, we consider the unpolarized DGLAP evolution of its collinear factor $f_{q/p}(x)$. Notice that in the SIDIS-1 fit we actually exploited also a different (powerlike) functional form for $h(k_\perp)$, still controlled by a single parameter, leading to almost no differences in our results. In what follows we will only use the functional form given in Eq. (12).

To reduce the number of free parameters, some additional assumptions were adopted. Concerning the SIDIS-1 fit, we considered only u and d quark Sivers functions, with flavor dependent α and β parameters. This amounts to a total of 7 parameters:

$$N_u, N_d, \alpha_u, \alpha_d, \beta_u, \beta_d, M. \tag{13}$$

In the SIDIS-2 fit, since we were aiming also at explaining some large kaon SIDIS azimuthal asymmetries, we tentatively included also the Sivers functions for antiquarks and strange quarks, $\bar{u}$, $\bar{d}$, s and $\bar{s}$. To keep the number of parameters under control we then assumed flavor independent α and β parameters for the sea quarks ($\alpha_{\rm sea}$, $\beta_{\rm sea}$). Moreover, since the large x behavior of the Sivers function could not, and still cannot, be constrained by SIDIS data (see a more detailed comment below), we also assumed a single flavor independent β parameter, equal for quarks and antiquarks. This amounts to a total of 11 free parameters:

$$N_u, N_d, N_{\bar{u}}, N_{\bar{d}}, N_s, N_{\bar{s}}, \alpha_u, \alpha_d, \alpha_{\rm sea}, \beta, M. \tag{14}$$

Notice that even with such a choice, our complete parametrization of the Sivers functions, Eq. (10), allows for further differences among parton flavors, which are contained in the usual unpolarized PDFs.

Both fits gave good results. Nevertheless it is worth stressing the main differences in the two extractions, which indeed play an important role in the present study. In fact, a direct use of SIDIS-1 results in the computation of SSAs in $p^\uparrow p \to hX$ processes for RHIC kinematics, as presented in Ref. [70], gave very encouraging results. Notice that at that time the Collins effect was believed to be suppressed [74]. On the other hand, if we use the SIDIS-2 fit to compute the same SSAs we would get too small A_N values, the reason being the different β values coming from the two fits.

More generally, as discussed in the context of the Collins SIDIS azimuthal asymmetries for the transversity distributions [71], a study of the statistical uncertainties of the best fit parameters clearly shows that SIDIS data are not presently able to constrain the large x behavior of the quark (u, d) Sivers distributions, leaving a large uncertainty in the possible values of the parameter β. This is due to the limited range of Bjorken x values currently explored by HERMES and COMPASS experiments, $x_B \lesssim 0.3$. In this respect the large x_B results expected from JLab 12 GeV experiments will be precious [80,81].

This uncertainty plays a crucial role when one tries to study the SSAs in hadronic collisions starting from the results obtained from SIDIS data, because the largest pion SSAs are measured at large Feynman x values, $x_F \gtrsim 0.3$, which implies $x \gtrsim 0.3$.

To investigate the role of the Sivers effect in explaining the large value of A_N in $p^\uparrow p$ collisions we should therefore carefully explore the large x behavior of the Sivers functions. To this aim we follow the same strategy we have devised in the recent study of the contribution of the Collins effect to A_N, the so-called "scan procedure" [71]. Here we summarize schematically its main steps and motivations.

(i) The β_q parameters, which control the large x behavior of the TMDs and are largely undetermined by SIDIS data, play instead an important role in the computation of A_N, which is sizable mainly in the large x_F region. We can notice this explicitly by comparing, as commented above, the different implications on A_N of the SIDIS-1 and the SIDIS-2 fits. In our choice of the independent parameters it is then natural to allow for a flavor dependence of β, limited, because of the relevance of the large x region, to the valence quark contributions. More explicitly, we only use the PDFs for u and d valence quarks in the Sivers functions (10), and the contribution of sea quarks and gluons is neglected in the sum over partons in Eq. (6).

(ii) We start the scan procedure by performing a preliminary 7-parameter [those of Eq. (13)] "reference fit" to SIDIS data. This reference best fit will have a total $\chi^2 = \chi^2_0$. We then let the two parameters β_u and β_d vary, choosing them in the range 0.0–4.0 by discrete steps of 0.5, and for each of the 81 pairs of fixed βs we perform a new 5-parameter fit to SIDIS data.

(iii) As a next step we select only those fits leading to a χ^2 such that $\chi^2 \leq \chi^2_0 + \Delta\chi^2$. Notice that, since the reference fit and the scan fits have a different number of free parameters, the selection criterion is applied to the total χ^2 rather than to the χ^2 per degree of freedom, $\chi^2_{\rm dof}$. The chosen value of $\Delta\chi^2$ is the same as that used to generate the error band, following the procedure described in Appendix A of Ref. [24]. We find (for 217 data points) $\chi^2_0 = 270.51$ and $\Delta\chi^2 = 14.34$. As expected from the arguments given above, all 81 fits lead to acceptable χ^2 values for SIDIS data; this further confirms the observation that the SIDIS data are not sensitive to the large x behavior of the Sivers function.

(iv) We then compute, for each of the 81 selected sets, the contribution of the Sivers effect to A_N,

according to Eqs. (4)–(6). We do that for pion and kaon production in the kinematical regions of the STAR and BRAHMS experiments at RHIC. The corresponding results span the shaded areas (scan band), which are shown in the figures of our results. When compared with the experimental available data, the scan bands show the potentiality of the Sivers effect alone to account for the measured values of A_N in $p^\uparrow p \to hX$ processes, while preserving a fair description (quantified by $\Delta\chi^2$) of the SIDIS data on the Sivers azimuthal asymmetry.

(v) We have considered in our scan procedure all available SIDIS data [82,83], with the exception of the recent ones by the COMPASS Collaboration off a transversely polarized proton target [84]. As shown in Refs. [16,17] the analysis of these data, reaching higher Q^2 values, requires a careful use of the proper TMD evolution, which is ignored here, as a correct implementation of the TMD evolution in $p^\uparrow p \to hX$ large P_T processes is so far unknown. We have checked that the $\chi^2_{\rm dof}$ of our fits would be approximately (30–40)% worse for the SIDIS data including the proton COMPASS results and no TMD evolution.

(vi) We study the contribution of the Sivers effect to the SSA A_N at RHIC energies only, although it might contribute also to the (larger) SSAs measured at lower energies [33–40]. The reason is that we consider only the processes for which our GPM and TMD factorization can reasonably well reproduce the unpolarized cross section [70].

1. Results from the scan procedure

Some of our results for RHIC experiments are shown in Figs. 1–4. We have computed A_N by adopting, as explained above, a single set of collinear parton distributions [77] and two different sets for the pion and kaon collinear FFs [76,78]; the results shown correspond to the Kretzer set. Other results not shown are very similar and would not add any significant information.

Let us start by considering the case of inclusive pion production. This will also help a direct comparison with the corresponding study on the potential role of the Collins contribution to the same observable [71].

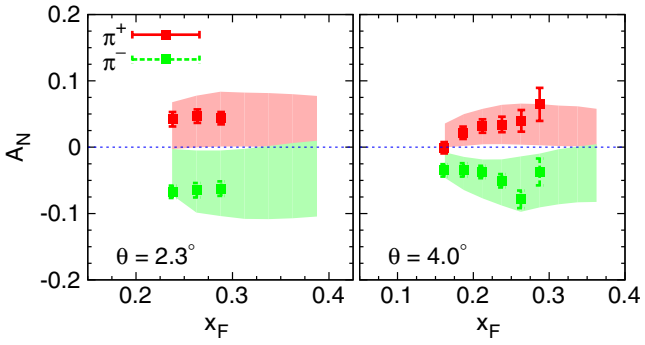

FIG. 1 (color online). Scan band (i.e. the envelope of the 81 curves obtained with the scanning procedure) for the Sivers contribution to the charged pion single spin asymmetries A_N, at $\sqrt{s} = 200$ GeV, as a function of x_F at two different scattering angles, compared with the corresponding BRAHMS experimental data [44]. The shaded scan band is generated, adopting the GRV98 set of collinear PDFs and the Kretzer FFs, following the procedure explained in the text.

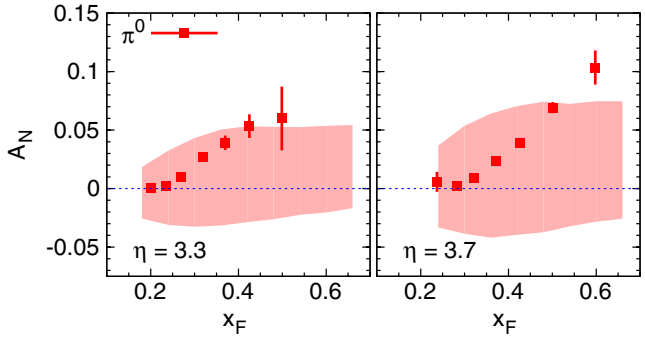

FIG. 2 (color online). Scan band (i.e. the envelope of the 81 curves obtained with the scanning procedure) for the Sivers contribution to the neutral pion single spin asymmetry A_N, at $\sqrt{s} = 200$ GeV, as a function of x_F at two different pseudorapidity values, compared with the corresponding STAR experimental data [45]. The shaded scan band is generated, adopting the GRV98 set of collinear PDFs and the Kretzer FFs, following the procedure explained in the text.

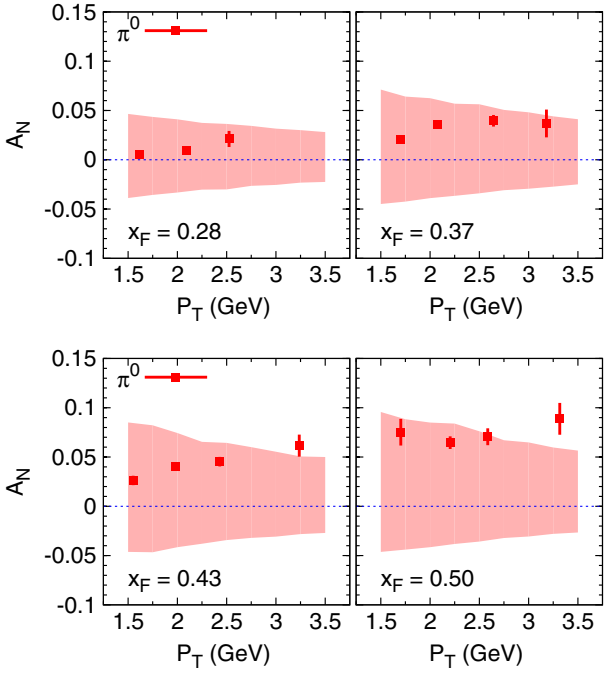

FIG. 3 (color online). The same as in Fig. 2, but with the STAR data plotted vs the pion transverse momentum, P_T, for different bins in x_F, $\langle x_F \rangle = 0.28$, 0.37, 0.43 and 0.50.

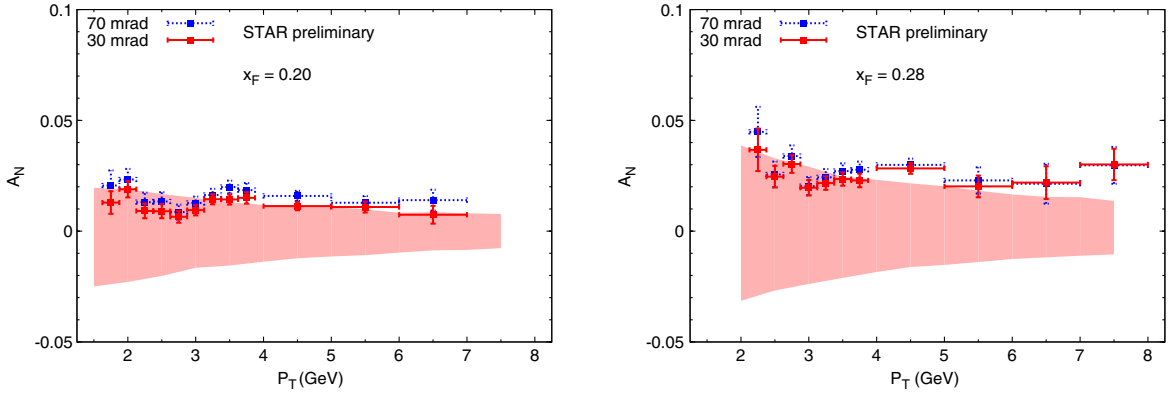

FIG. 4 (color online). Scan band (i.e. the envelope of the 81 curves obtained with the scanning procedure) for the Sivers contribution to the neutral pion single spin asymmetry A_N, as a function of P_T for different x_F values at $\sqrt{s} =$ 500 GeV, compared with the corresponding STAR preliminary experimental data at $\langle x_F \rangle = 0.20,\ 0.28$ [47]. The shaded scan band is generated, adopting the GRV98 set of collinear PDFs and the Kretzer FF set, following the procedure explained in the text.

In Fig. 1 the scan band for A_N, as a function of x_F at fixed scattering angles, is shown for charged pions and BRAHMS kinematics, while in Fig. 2 the same result is given, at fixed pseudorapidity values, for neutral pions and STAR kinematics. We also give the scan band, as a function of P_T at several fixed x_F values, for STAR kinematics in Fig. 3. All these results are given at $\sqrt{s} = 200$ GeV. We then consider the latest and interesting preliminary data obtained by STAR at large P_T and $\sqrt{s} = 500$ GeV [47], and show our scan band in Fig. 4 for different values of x_F.

From these results we can conclude that the Sivers effect alone might in principle be able to explain the BRAHMS charged pion results on A_N in the full kinematical range so far explored, as well as almost the full amount of STAR π^0 data on A_N. This is to be contrasted with the analogous study of the Collins effect [71], with the conclusion that such an effect alone cannot explain the observed values of A_N in the medium-large x_F region.

This can be understood as follows. In the case of SSAs for neutral pion production the Collins effect suffers from two possible cancellations: the opposite sign between the u and d quark transversity distributions and the opposite sign between the favored and disfavored Collins FFs (necessary to build the Collins FF for π^0); instead, for the Sivers effect only a cancellation between u and d flavors in the distribution sector may play a role, as it couples to the unpolarized TMD-FF.

A further remark concerns the values of the β parameters and the area spanned by the bands: the upper borderlines of the scan bands for neutral and positively charged pions correspond to the set of Sivers functions with $\beta_u = 0$ (up quark unsuppressed) and $\beta_d = 4$ (down quark strongly suppressed), while the lower borderlines correspond to the case where the values of β are interchanged. Notice that larger values of β would not change this picture. For negative pions the situation is just reversed since to get the largest values, in size, of A_N (lower border) the down quark should dominate (that is $\beta_d = 0$ and $\beta_u = 4$).

The results obtained with a different choice of the fragmentation functions (the DSS set) are qualitatively very similar in the large x_F regions. They are instead smaller in size at smaller x_F, due to the large gluon contribution in the leading order (LO) DSS fragmentation functions. They are not shown here.

The case of SSAs for kaon production would require a further study of the corresponding unpolarized fragmentation functions, which represents an open issue by itself and falls outside the purposes of this paper. However, for completeness and a qualitative estimate, we consider A_N for $K^{\pm}$ production as measured by the BRAHMS Collaboration [44], with the kaon set of fragmentation function as given in Ref. [76]. Our results for the scan band, compared with the data, are shown in Fig. 5.

The results in Figs. 1–5 show that the Sivers effect alone, as computed in our GPM scheme, Eqs. (4)–(6), and based

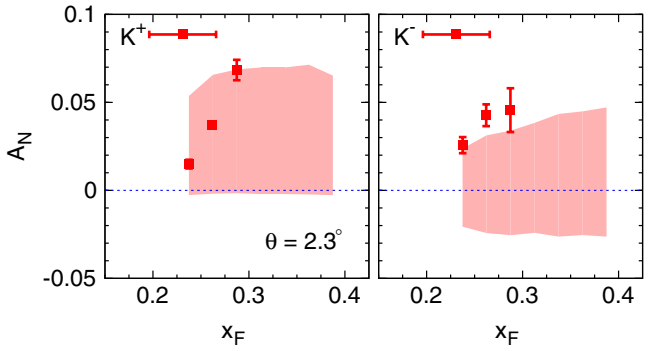

FIG. 5 (color online). Scan band (i.e. the envelope of the 81 curves obtained with the scanning procedure) for the Sivers contribution to the kaon single spin asymmetry A_N, as a function of x_F, at $\sqrt{s} = 200$ GeV and a fixed scattering angle, compared with the corresponding BRAHMS experimental data [44]. The shaded scan band is generated, adopting the GRV98 set of collinear PDFs and the Kretzer FF set, following the procedure explained in the text.

on the Sivers functions extracted from SIDIS data and assumed to be universal, can be large enough to explain alone the pion SSAs A_N observed at RHIC. One should not forget that, indeed, the phenomenology of the Sivers effect was originally generated in the attempt to explain the large values of A_N observed by the E704 Collaboration [1,2,62]. However, the amount of uncertainty in the scan bands, due to the lack of precise SIDIS data at large x, is still much too large to draw any definite conclusions.

A full understanding of the SSAs in inclusive $p^\uparrow p \to hX$ processes should also take into account the contribution of the Collins effect, which might be small, but not entirely negligible. Rather than addressing the issue of a best fit of SIDIS + A_N data with Collins and Sivers effects, which is premature at this stage, we now adopt a more pragmatic attitude. We wonder whether, among the 81 sets of parameters that build up the possible results on A_N contained in the scan bands, we can find some that give a good description of all the data.

2. Results with a selected set of parameters and its statistical uncertainty bands

Among the full set of curves produced by the scan procedure, we have isolated the set leading to the best description of A_N (actually one could find more than a single set); we have then evaluated, as in Appendix A of Ref. [24], the corresponding statistical error band. Our results are presented in Figs. 6–9, respectively, for BRAHMS $\pi^\pm$ data vs x_F at fixed angles, for STAR π^0 results vs x_F at fixed pseudorapidities, for STAR π^0 results vs P_T at different x_F values, and for BRAHMS $K^\pm$ data vs x_F at a fixed angle, all of them at $\sqrt{s} = 200$ GeV. The corresponding values of the parameters are given in Table I. From these results one can see that it is possible

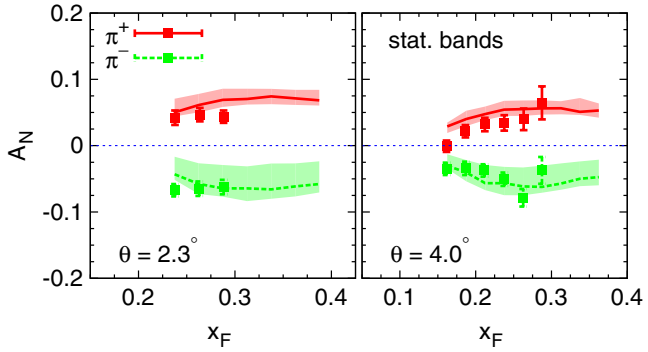

FIG. 6 (color online). The Sivers contribution to the charged pion single spin asymmetry A_N, compared with the corresponding BRAHMS experimental data at two fixed scattering angles and $\sqrt{s} = 200$ GeV [44]. The central lines are obtained adopting the GRV98 set of collinear PDFs and the Kretzer FFs, with the Sivers functions as in Eqs. (10)–(12) with the parameters given in Table I. The shaded statistical error bands are generated applying the error estimate procedure described in Appendix A of Ref. [24].

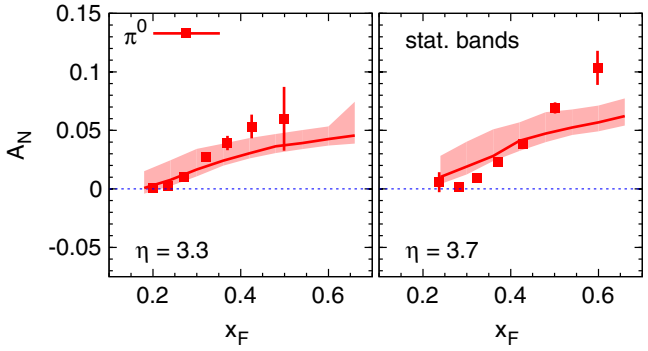

FIG. 7 (color online). The Sivers contribution to the neutral pion single spin asymmetry A_N, compared with the corresponding STAR experimental data at two fixed pion rapidities and $\sqrt{s} = 200$ GeV [45]. The central lines are obtained adopting the GRV98 set of collinear PDFs and the Kretzer FFs, with the Sivers functions as in Eqs. (10)–(12) with the parameters given in Table I. The shaded statistical error bands are generated applying the error estimate procedure described in Appendix A of Ref. [24].

to find a set of Sivers functions for u and d quarks that, while describing well the SIDIS data, can also describe fairly well, alone, the SSAs for pion production, as measured by both BRAHMS and STAR Collaborations at 200 GeV.

The preliminary STAR data at 500 GeV [47] deserve a dedicated comment. Quite surprisingly, they show values

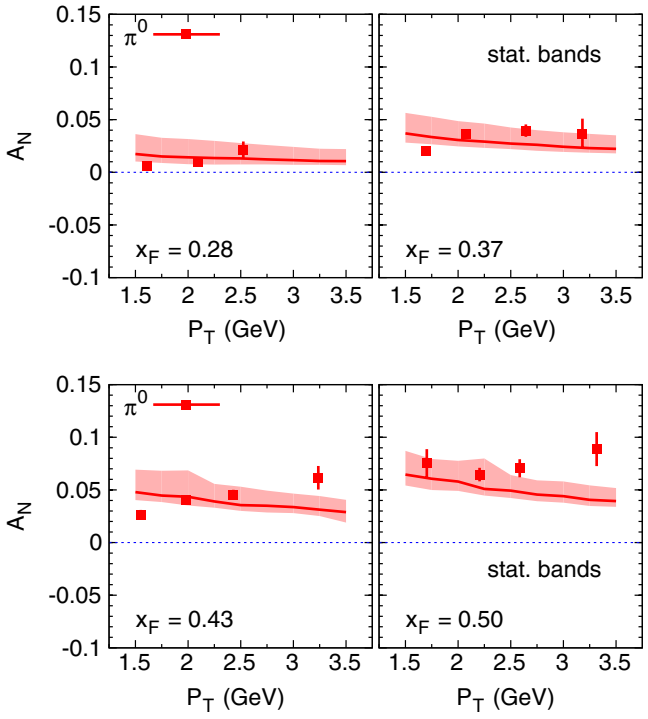

FIG. 8 (color online). The same as in Fig. 7, but with the STAR data plotted vs the pion transverse momentum, P_T, for different bins in x_F, $\langle x_F \rangle = 0.28$, 0.37, 0.43 and 0.50.

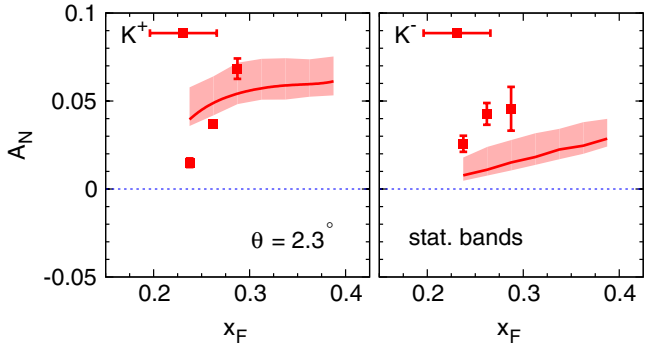

FIG. 9 (color online). The Sivers contribution to the charged kaon single spin asymmetry A_N, compared with the corresponding BRAHMS experimental data at a fixed scattering angle and $\sqrt{s} = 200$ GeV [44]. The central lines are obtained adopting the GRV98 set of collinear PDFs and the Kretzer FFs, with the Sivers functions as in Eqs. (10)–(12) with the parameters given in Table I. The shaded statistical error bands are generated applying the error estimate procedure described in Appendix A of Ref. [24].

of A_N of the order of a few percent, with a flat behavior as a function of P_T at fixed x_F, up to $P_T \simeq 7$ GeV. Such a trend is well reproduced by our set of chosen best parameters; however, the computed magnitude of A_N is smaller than data, as shown in Fig. 10, left plots. As the asymmetry is so small, we have also computed the Collins contribution to A_N, following Ref. [71]. It turns out that, for some sets of the parameters, the Collins contribution has a similar trend and magnitude as the Sivers one, as shown in Fig. 10, right plots. Then, an appropriate sum of the two contributions, according to Eq. (5), might well explain also this new puzzling data.

Another cautious comment about the STAR data on A_N at 500 GeV concerns the large value of their QCD scale, $Q^2 = P_T^2$. As we noticed for the COMPASS proton data, at such values the TMD evolution might play an important role. Our results should then be taken as an indication in favor of a combined Collins + Sivers effect, rather than a proof. Qualitatively, one expects from TMD evolution an increase of the average $\langle k_\perp^2 \rangle$ value of the Sivers distribution, which would help increase the corresponding value of A_N.

B. SSAs for $p^\uparrow p \to$ jet X and $p^\uparrow p \to \gamma X$ processes

In these processes no fragmentation mechanism is required, so that, within the GPM and the TMD factorization approach, one can access directly the spin and $\boldsymbol{k}_\perp$ properties of the partonic distributions. After integration over the intrinsic azimuthal phases, only the Sivers effect survives,

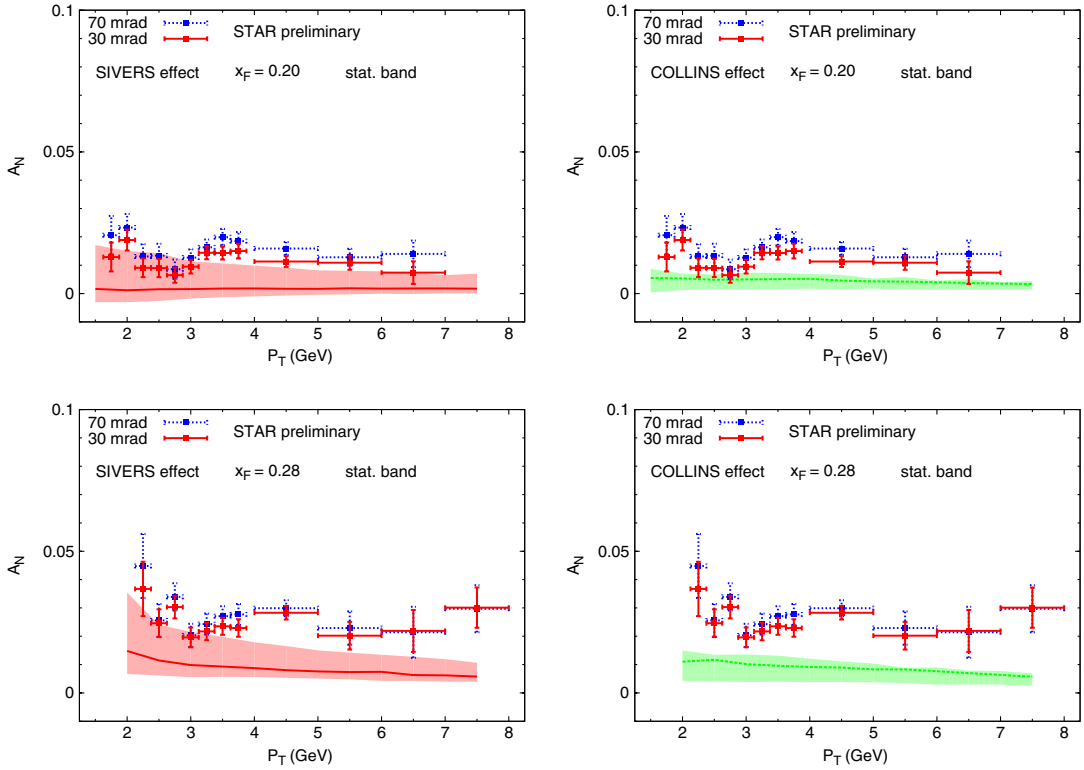

FIG. 10 (color online). Left panels: the Sivers contribution to the π^0 single spin asymmetry A_N vs the pion transverse momentum P_T, for different bins in x_F, compared with the corresponding STAR preliminary data at $\sqrt{s} = 500$ GeV and $\langle x_F \rangle = 0.20, 0.28$ [47]. The central lines are obtained adopting the GRV98 set of collinear PDFs and the Kretzer FFs, with the Sivers functions as in Eqs. (10)–(12) with the parameters given in Table I. The shaded statistical error bands are generated applying the error estimate procedure described in Appendix A of Ref. [24]. Right panels: the Collins contribution to the same A_N, computed according to Ref. [71], choosing the Collins functions, among those of the scan band, which give the maximum contribution.

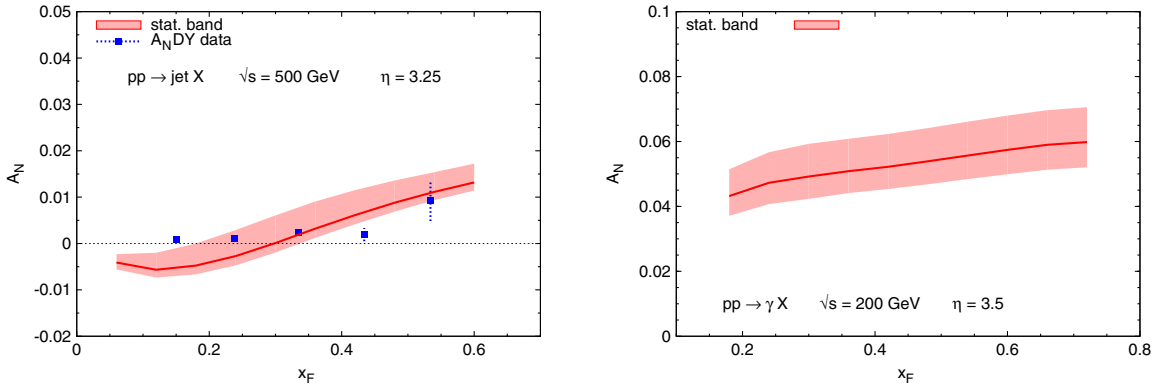

FIG. 11 (color online). Left panel: our estimate for the jet SSA A_N at $\sqrt{s} = 500$ GeV, as a function of x_F at fixed pseudorapidity $\eta = 3.25$, compared with the A_NDY data [48]. The central line is obtained adopting the GRV98 set of collinear PDFs, with the Sivers functions as in Eqs. (10)–(12) with the parameters given in Table I. The shaded statistical error band is generated applying the error estimate procedure described in Appendix A of Ref. [24]. Right panel: the same estimate as in the left panel for a direct photon, rather than a jet, production at $\sqrt{s} = 200$ GeV and $\eta = 3.5$.

which is then best studied in these processes, as discussed, e.g., in Refs. [65,85]. Notice that, for the same reasons, the SSAs for inclusive jet or photon production can be used to test the process dependence of the Sivers functions in a modified generalized parton model with the inclusion of initial and final state interactions [68,86] or within the twist-3 approach [60].

The numerator of A_N for the inclusive jet production can be obtained from Eq. (6) simply by replacing the TMD fragmentation function, $D_{h/c}(z, p_\perp)$, with a factor $\delta(z-1)\delta^2(\boldsymbol{p}_\perp)$ (and identifying now the final hadron momentum, $\boldsymbol{p}_h$, with the jet momentum $\boldsymbol{p}_c \equiv \boldsymbol{p}_{\rm jet}$). More explicitly the numerator of A_N for inclusive jet production reads

$$[d\sigma^\uparrow - d\sigma^\downarrow]^{p^\uparrow p\to {\rm jet}X}_{\rm Sivers} = \sum_{a,b,c,d}\int \frac{dx_a dx_b}{16\pi^2 x_a x_b s} d^2\boldsymbol{k}_{\perp a} d^2\boldsymbol{k}_{\perp b}\delta(\hat{s}+\hat{t}+\hat{u}) \times \Delta^N f_{a/p^\uparrow}(x_a, k_{\perp a})\cos(\phi_a) f_{b/p}(x_b, k_{\perp b})\frac{1}{2}[|\hat{M}_1^0|^2 + |\hat{M}_2^0|^2 + |\hat{M}_3^0|^2]_{ab\to cd}. \quad (15)$$

Notice that the elementary hard scattering interactions are exactly the same as those for the inclusive hadron production and the jet, at LO, is identified with the final parton c.

Concerning the direct photon production the basic partonic processes are the Compton process $gq(\bar{q}) \to \gamma q(\bar{q})$ and the annihilation process $q\bar{q} \to \gamma g$. In this case one can formally use the above equation replacing the partonic unpolarized cross section, Eq. (7), with the corresponding one for the process $ab \to \gamma d$ (see also Ref. [65]).

No SSA data are so far available for direct photon production, while very recently some preliminary data for inclusive jet production have been released by the A_NDY Collaboration at $\sqrt{s} = 500$ GeV [48]. The values measured for A_N are very tiny, but very precise and might indicate a nonzero asymmetry.

In the left plot of Fig. 11 we show our estimate, based on the chosen best set parameters of Table I, for $A_N(x_F)$ in $p^\uparrow p \to {\rm jet}\, X$ processes at a fixed pseudorapidity value and $\sqrt{s} = 500$ GeV, and compare it with the A_NDY data [48]. In the right plot we give our corresponding estimates for $A_N(x_F)$ in $p^\uparrow p \to \gamma X$ processes at a fixed pseudorapidity value and $\sqrt{s} = 200$ GeV.

For consistency, in Fig. 12 we compare our (leading order) computation of the cross section for jet production as given by Eq. (15) where we replace the factor $\Delta^N f_{a/p^\uparrow}\cos(\phi_a)$ with $f_{a/p}$, with the A_NDY data at $\sqrt{s} = 510$ GeV and fixed pseudorapidity $\eta = 3.25$.

TABLE I. Our chosen set of seven parameters, Eq. (13), fixing the u and d quark Sivers distribution functions, according to Eqs. (10)–(12). Among the 81 sets of the scan procedure, this set gives the best description of the A_N data. The corresponding total value of χ^2 for the 217 SIDIS data points is 273.2, which is very close to the best value $\chi^2_0 = 270.5$ of the reference set. The statistical errors quoted for each free parameter correspond to the shaded uncertainty areas in Figs. 6–9 and 11 and the left panels of Fig. 10, as explained in the text and in the Appendix of Ref. [24].

$N_u = 0.35^{+0.08}_{-0.04}$	$\alpha_u = 0.00^{+0.06}_{-0.00}$	$\beta_u = 0.00$
$N_d = -1.00^{+0.24}_{-0.00}$	$\alpha_d = 0.24^{+0.11}_{-0.17}$	$\beta_d = 1.00$
$M^2 = 0.44^{+0.78}_{-0.15}$ GeV^2		

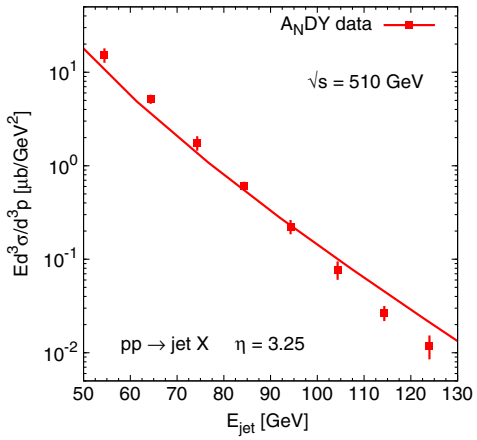

FIG. 12 (color online). Our computation of the unpolarized cross section for jet production vs the jet energy, at $\sqrt{s} = 510$ GeV and fixed pseudorapidity $\eta = 3.25$, compared with A_NDY data [48].

III. CONCLUSIONS

The origin of the azimuthal asymmetries in SIDIS processes is considered to be well understood and related to TMD-PDFs and TMD-FFs, via the QCD TMD factorization scheme. Indeed, the measurement of such asymmetries has been used to extract information on the TMDs. A reasonable knowledge of the Sivers TMD-PDF is by now available and confirmed by independent groups [23–27]. However, because of the kinematical range of the data, this knowledge is limited to the small x region, $x \lesssim 0.3$. The same TMD factorization is expected to hold also in Drell-Yan and $e^+e^- \to h_1 h_2 X$ processes.

The situation is not so clear concerning the oldest and largest single spin asymmetries A_N measured in several hadronic processes, in particular in $p^\uparrow p \to hX$. Because of the presence of a single large scale—the P_T of the final hadron—one cannot extend to these processes the proof of the QCD TMD factorization theorem, which requires the presence of two separate scales, a large and a small one. As explained in the Introduction, a twist-3 collinear and factorized approach has been proposed [49–57], which introduces new three-parton correlation functions, related to the $k_\perp$ moment of the TMD-PDFs. However, it seems to predict values of A_N opposite to the observed ones [59]. Thus, the true origin of the large values of A_N remains obscure.

Among the first attempts to explain A_N [1,2,62–67], and the unpolarized cross section [73], one should consider the simple extension of the collinear QCD factorization to the TMD case, the so-called GPM in which one assumes TMD factorization and the universality of the TMF-PDFs and TMD-FFs. Although such a factorization has not been proven, it is worth exploring its phenomenological consequences. In this paper we have studied, within the GPM, the contribution of the Sivers effect to the single spin asymmetry A_N as measured by RHIC Collaboration experiments. The Sivers functions are the same as those that explain azimuthal asymmetries in SIDIS processes. A similar analysis was performed in Ref. [71], concerning the Collins effect.

Our results, limited to the contribution of the valence quarks, to the SIDIS cases where the TMD evolution is not expected to be relevant and to the $pp \to \pi X$ large P_T processes for which we can well reproduce the unpolarized cross sections, are rather encouraging. For most pion data the Sivers effect alone could explain the observed values of A_N in magnitude and, in particular, in sign. This is in contrast to other approaches, also related to the Sivers effect, which seem to have severe problems [59,68] in explaining the sign of the observed A_N.

We have performed our analysis by varying the parameters of the Sivers functions that are not well fixed by the SIDIS data, due to their limited kinematical range, obtaining the so-called scan bands. In particular, we have let the power β that fixes the large x behavior of the u and d quark Sivers functions, $(1-x)^\beta$, vary between 0 and 4 in steps of 0.5. Thus, we have 81 different sets of Sivers functions; each of them still fits well the SIDIS data. The bands, which appear in Figs. 1–5, are the envelope of the 81 different curves, $A_N(x_F)$ and $A_N(P_T)$, obtained in our GPM approach.

Then, among the explored sets of parameters, we have chosen a particular one, which gives one of the best descriptions of the A_N data. We have used such a set to compute estimates for SSAs in $p^\uparrow p \to \text{jet}\, X$ and $p^\uparrow p \to \gamma X$ processes. Such measurements will further allow one to discriminate between our approach and others. Predictions for A_N in different processes and kinematical regions can be easily obtained, if necessary.

While encouraged by the results of our analysis we should avoid making definite conclusions at this stage. This work shows that the GPM TMD factorization scheme could explain at the same time the main features of the SSAs measured in SIDIS and hadronic processes. While such a scheme is well justified for SIDIS it can, so far, only be considered as a phenomenological model for hadronic processes, which needs further confirmation or disproval from data and further theoretical work. Our choice of the sets of parameters given in Table I is not meant to be interpreted as the final best set of Sivers functions. A full analysis, including TMD evolution, of all data involving the Sivers effect—i.e. all the SSAs in several different processes—would require much more attention and work.

ACKNOWLEDGMENTS

We would like to thank L. Bland for information on the A_NDY data and S. Heppelmann for information on the STAR data on A_N at 500 GeV. We acknowledge support of the European Community under the FP7

''Capacities—Research Infrastructures'' program (HadronPhysics3, Grant Agreement No. 283286). Some of us (M. A., M. B., U. D., F. M.) acknowledge partial support from MIUR under Cofinanziamento PRIN 2008. U. D. is grateful to the Department of Theoretical Physics II of the Universidad Complutense of Madrid for the kind hospitality extended to him during the completion of this work.

[1] D. W. Sivers, Phys. Rev. D **41**, 83 (1990).
[2] D. W. Sivers, Phys. Rev. D **43**, 261 (1991).
[3] D. Boer and P. Mulders, Phys. Rev. D **57**, 5780 (1998).
[4] P. J. Mulders and R. D. Tangerman, Nucl. Phys. **B461**, 197 (1996).
[5] A. Bacchetta, U. D'Alesio, M. Diehl, and C. A. Miller, Phys. Rev. D **70**, 117504 (2004).
[6] D. Boer *et al.*, arXiv:1108.1713.
[7] A. Bacchetta and M. Radici, Phys. Rev. Lett. **107**, 212001 (2011).
[8] X.-d. Ji, J.-P. Ma, and F. Yuan, Phys. Lett. B **597**, 299 (2004).
[9] X.-d. Ji, J.-p. Ma, and F. Yuan, Phys. Rev. D **71**, 034005 (2005).
[10] A. Bacchetta, D. Boer, M. Diehl, and P. J. Mulders, J. High Energy Phys. 08 (2008) 023.
[11] J. Collins, *Foundations of Perturbative QCD*, Cambridge Monographs on Particle Physics, Nuclear Physics and Cosmology Vol. 32 (Cambridge University Press, Cambridge, 2011).
[12] S. M. Aybat and T. C. Rogers, Phys. Rev. D **83**, 114042 (2011).
[13] S. M. Aybat, J. C. Collins, J.-W. Qiu, and T. C. Rogers, Phys. Rev. D **85**, 034043 (2012).
[14] M. G. Echevarria, A. Idilbi, A. Schafer, and I. Scimemi, arXiv:1208.1281.
[15] M. G. Echevarria, A. Idilbi, and I. Scimemi, Int. J. Mod. Phys. Conf. Ser. **20**, 92 (2012).
[16] S. M. Aybat, A. Prokudin, and T. C. Rogers, Phys. Rev. Lett. **108**, 242003 (2012).
[17] M. Anselmino, M. Boglione, and S. Melis, Phys. Rev. D **86**, 014028 (2012).
[18] A. Bacchetta and A. Prokudin, Nucl. Phys. **B875**, 536 (2013).
[19] R. M. Godbole, A. Misra, A. Mukherjee, and V. S. Rawoot, Phys. Rev. D **88**, 014029 (2013).
[20] P. Sun and F. Yuan, Phys. Rev. D **88**, 034016 (2013).
[21] D. Boer, Nucl. Phys. **B874**, 217 (2013).
[22] P. Sun and F. Yuan, arXiv:1308.5003.
[23] M. Anselmino, M. Boglione, U. D'Alesio, A. Kotzinian, F. Murgia, and A. Prokudin, Phys. Rev. D **72**, 094007 (2005); **72**, 099903(E) (2005).
[24] M. Anselmino, M. Boglione, U. D'Alesio, A. Kotzinian, S. Melis, F. Murgia, A. Prokudin, and C. Turk, Eur. Phys. J. A **39**, 89 (2009).
[25] W. Vogelsang and F. Yuan, Phys. Rev. D **72**, 054028 (2005).
[26] J. C. Collins, A. V. Efremov, K. Goeke, S. Menzel, A. Metz, and P. Schweitzer, Phys. Rev. D **73**, 014021 (2006).
[27] M. Anselmino *et al.*, in *Proceedings of the International Workshop on Transverse Polarization Phenomena in Hard Processes (Transversity 2005), Como, Italy, 2005*, edited by V. Barone and P. G. Ratcliffe (World Scientific, Singapore, 2006), p. 236.
[28] M. Diefenthaler (HERMES Collaboration), arXiv:0706.2242.
[29] A. Martin (COMPASS Collaboration), Czech. J. Phys. **56**, F33 (2006).
[30] S. J. Brodsky, D. S. Hwang, and I. Schmidt, Phys. Lett. B **530**, 99 (2002).
[31] S. J. Brodsky, D. S. Hwang, and I. Schmidt, Nucl. Phys. **B642**, 344 (2002).
[32] J. C. Collins, Phys. Lett. B **536**, 43 (2002).
[33] R. D. Klem, J. E. Bowers, H. W. Courant, H. Kagan, M. L. Marshak, E. A. Peterson, K. Ruddick, W. H. Dragoset, and J. B. Roberts, Phys. Rev. Lett. **36**, 929 (1976).
[34] K. Krueger *et al.*, Phys. Lett. B **459**, 412 (1999).
[35] C. Allgower *et al.*, Phys. Rev. D **65**, 092008 (2002).
[36] J. Antille, L. Dick, L. Madansky, D. Perret-Gallix, M. Werlen, A. Gonidec, K. Kuroda, and P. Kyberd, Phys. Lett. **94B**, 523 (1980).
[37] D. L. Adams *et al.* (E581 Collaboration and E704 Collaboration), Phys. Lett. B **261**, 201 (1991).
[38] D. L. Adams *et al.* (E704 Collaboration), Phys. Lett. B **264**, 462 (1991).
[39] D. L. Adams *et al.* (E581 Collaboration and E704 Collaboration), Phys. Lett. B **276**, 531 (1992).
[40] D. L. Adams *et al.* (E581 Collaboration and E704 Collaboration), Z. Phys. C **56**, 181 (1992).
[41] I. Arsene *et al.* (BRAHMS Collaboration), Phys. Rev. Lett. **101**, 042001 (2008).
[42] J. Adams *et al.* (STAR Collaboration), Phys. Rev. Lett. **92**, 171801 (2004).
[43] S. S. Adler *et al.* (PHENIX Collaboration), Phys. Rev. Lett. **95**, 202001 (2005).
[44] J. H. Lee and F. Videbaek (BRAHMS Collaboration), AIP Conf. Proc. **915**, 533 (2007).
[45] B. Abelev *et al.* (STAR Collaboration), Phys. Rev. Lett. **101**, 222001 (2008).
[46] L. Adamczyk *et al.* (STAR Collaboration), Phys. Rev. D **86**, 051101 (2012).
[47] G. Igo (for the STAR Collaboration), AIP Conf. Proc. **1523**, 188 (2013).
[48] L. Bland *et al.* (AnDY Collaboration), arXiv:1304.1454.
[49] A. V. Efremov and O. V. Teryaev, Yad. Fiz. **36**, 242 (1982) [Sov. J. Nucl. Phys. **36**, 140 (1982)].
[50] A. V. Efremov and O. V. Teryaev, Phys. Lett. **150B**, 383 (1985).
[51] J.-w. Qiu and G. Sterman, Phys. Rev. Lett. **67**, 2264 (1991).

[52] J.-w. Qiu and G. Sterman, Phys. Rev. D **59**, 014004 (1998).
[53] Y. Kanazawa and Y. Koike, Phys. Lett. B **478**, 121 (2000).
[54] Y. Kanazawa and Y. Koike, Phys. Lett. B **490**, 99 (2000).
[55] C. Kouvaris, J.-W. Qiu, W. Vogelsang, and F. Yuan, Phys. Rev. D **74**, 114013 (2006).
[56] K. Kanazawa and Y. Koike, Phys. Rev. D **82**, 034009 (2010).
[57] K. Kanazawa and Y. Koike, Phys. Rev. D **83**, 114024 (2011).
[58] D. Boer, P. J. Mulders, and F. Pijlman, Nucl. Phys. **B667**, 201 (2003).
[59] Z.-B. Kang, J.-W. Qiu, W. Vogelsang, and F. Yuan, Phys. Rev. D **83**, 094001 (2011).
[60] L. Gamberg, Z.-B. Kang, and A. Prokudin, Phys. Rev. Lett. **110**, 232301 (2013).
[61] L. Nogach (AnDY Collaboration), arXiv:1212.3437.
[62] M. Anselmino, M. Boglione, and F. Murgia, Phys. Lett. B **362**, 164 (1995).
[63] M. Anselmino and F. Murgia, Phys. Lett. B **442**, 470 (1998).
[64] M. Anselmino, M. Boglione, and F. Murgia, Phys. Rev. D **60**, 054027 (1999).
[65] U. D'Alesio and F. Murgia, Phys. Rev. D **70**, 074009 (2004).
[66] M. Anselmino, M. Boglione, U. D'Alesio, E. Leader, S. Melis, and F. Murgia, Phys. Rev. D **73**, 014020 (2006).
[67] U. D'Alesio and F. Murgia, Prog. Part. Nucl. Phys. **61**, 394 (2008).
[68] L. Gamberg and Z.-B. Kang, Phys. Lett. B **696**, 109 (2011).
[69] P. G. Ratcliffe and O. V. Teryaev, arXiv:0911.4306.
[70] M. Boglione, U. D'Alesio, and F. Murgia, Phys. Rev. D **77**, 051502 (2008).
[71] M. Anselmino, M. Boglione, U. D'Alesio, E. Leader, S. Melis, F. Murgia, and A. Prokudin, Phys. Rev. D **86**, 074032 (2012).
[72] J. C. Collins, Nucl. Phys. **B396**, 161 (1993).
[73] R. P. Feynman, R. D. Field, and G. C. Fox, Phys. Rev. D **18**, 3320 (1978).
[74] M. Anselmino, M. Boglione, U. D'Alesio, E. Leader, and F. Murgia, Phys. Rev. D **71**, 014002 (2005).
[75] A. Martin, R. Roberts, W. Stirling, and R. Thorne, Phys. Lett. B **531**, 216 (2002).
[76] S. Kretzer, Phys. Rev. D **62**, 054001 (2000).
[77] M. Gluck, E. Reya, and A. Vogt, Eur. Phys. J. C **5**, 461 (1998).
[78] D. de Florian, R. Sassot, and M. Stratmann, Phys. Rev. D **75**, 114010 (2007).
[79] M. Anselmino, M. Boglione, U. D'Alesio, A. Kotzinian, F. Murgia, and A. Prokudin, Phys. Rev. D **71**, 074006 (2005).
[80] H. Gao *et al.*, Eur. Phys. J. Plus **126**, 2 (2011).
[81] H. Gao, J.-P. Chen, M. Huang, and X. Qian, J. Phys. Conf. Ser. **295**, 012019 (2011).
[82] A. Airapetian *et al.* (HERMES Collaboration), Phys. Rev. Lett. **103**, 152002 (2009).
[83] M. Alekseev *et al.* (COMPASS Collaboration), Phys. Lett. B **673**, 127 (2009).
[84] C. Adolph *et al.* (COMPASS Collaboration), Phys. Lett. B **717**, 383 (2012).
[85] U. D'Alesio, F. Murgia, and C. Pisano, Phys. Rev. D **83**, 034021 (2011).
[86] U. D'Alesio, L. Gamberg, Z.-B. Kang, F. Murgia, and C. Pisano, Phys. Lett. B **704**, 637 (2011).